Characterization of ascites-derived aldehyde dehydrogenase–positive ovarian cancer stem cells isolated from Leghorn chickens

Anupama Tiwari,* Jill A. Hadley,* and Ramesh Ramachandran*,[1]

*Center for Reproductive Biology and Health, Department of Animal Science, The Pennsylvania State University, University Park, PA

ABSTRACT Leghorn chickens are used as a preclinical model of ovarian cancer as they develop epithelial ovarian adenocarcinoma spontaneously at a very high frequency. Ovarian cancer is the most lethal disease among all gynecological malignancies in women. A small proportion of ovarian cancer stem cells are responsible for drug resistance and relapse of ovarian cancer. The objectives of this study are to isolate ovarian cancer stem cells from ascites of Leghorn chickens that spontaneously developed ovarian cancer and to determine their invasiveness, spheroid formation in three-dimensional culture devoid of extracellular matrix over several months. Ovarian cancer cells obtained from ascites were subjected to ALDEFLOUR assay that measures aldehyde dehydrogenase (**ALDH**) activity to separate ALDH1$^+$ and ALDH1$^-$ cells by fluorescence-activated cell sorting. The cells were cultured using serum-free media for up to 6 mo in ultra-low attachment plates. Invasiveness of ALDH1$^+$ and ALDH1$^-$ cells was determined by Matrigel invasion assay. Cellular uptake of acetylated low-density lipoprotein was evaluated. A small proportion (<4.75%) of ovarian cancer cells isolated from ascites were found to be ALDH1$^+$ cells. ALDH1$^+$ cells formed a greater number of spheroids and were also highly invasive in extracellular matrix compared to ALDH1$^-$ cells. Several spheroids developed 0.1- to 1-mm-long capillary-like tubules connecting other spheroids, thus forming a complex network that underwent remodeling over several months. Cells in the spheroids incorporated acetylated low-density lipoprotein suggestive of scavenger receptor activity. In summary, ALDH1$^+$ ovarian cancer stem cells isolated from ascites of chickens appear to be invasive and form spheroids with complex networks of tubules reminiscent of vascular mimicry. Understanding the structure and function of spheroids and tubular network would provide valuable insight into the biology of ovarian cancer and improve poultry health.

Key words: chicken model of ovarian cancer, cancer stem cell, spheroid formation, invasiveness, vascular mimicry

2020 Poultry Science 99:2203–2214
https://doi.org/10.1016/j.psj.2019.11.052

INTRODUCTION

Ovarian cancer is the most lethal gynecological malignancy in women. The American Cancer Society estimates that approximately 22,530 new cases of ovarian cancer will be diagnosed, and approximately 13,980 women are likely to die due to this disease in the United States in the year 2019. The higher rate of mortality is attributed to the fact that women with ovarian cancer do not exhibit symptoms at an early stage but are often (>85% of cases) diagnosed at advanced stages of disease progression resulting in a poor (27%) 5-y survival rate. The aggressive behavior of ovarian adenocarcinoma is partly attributable to the existence of a small population of progenitor-like ovarian cancer stem cells typically found in the ascites of advanced stages of ovarian cancer (Bapat et al., 2005). Cancer stem cells are resistant to chemotherapy but have the ability to self-renew and differentiate, leading to tumor relapse and metastasis (Jordan et al., 2006). Recurrent ovarian adenocarcinomatous tissues are enriched with cancer stem cells and stem cell pathway mediators such as aldehyde dehydrogenase (**ALDH1**), CD133, CD44, Notch, Wnt, and transforming growth factor-β (Steg et al., 2012). The biology of ovarian cancer stem cells is poorly understood, especially when they exist in ascites. The present study is attempting to fill this gap in knowledge by using an ovarian cancer model that spontaneously develops ovarian cancer.

Leghorn chickens are the only animal model that develops ovarian cancer naturally that closely resembles human ovarian cancer (Fredrickson, 1987; Johnson and

Received August 20, 2019.
Accepted November 19, 2019.

[1]Corresponding author: RameshR@psu.edu

Giles, 2013; Lengyel et al., 2014). Although the cause of spontaneous ovarian cancer is unknown, incessant ovulation (Fathalla, 1971) is associated with a high rate of ovarian cancer incidence. Modern-day Leghorn chickens are the most efficient egg producers and lay approximately 300 eggs per year and, therefore, ovulate almost daily between 6 mo and 18 mo of age. A high proportion (25-40%) of hens aged between 2 and 4 yr develop epithelial ovarian adenocarcinoma (Campbell, 1951; Lingeman, 1974; Fredrickson, 1987; Barnes et al., 2002). The cancer cells from ovarian tumor in chickens, as in women, metastasizes to various visceral organs including peritoneum (Tiwari et al., 2013), and such progression is classified into stages I-IV (Barua et al., 2009). We found that, as in women, stages III and IV of ovarian cancer in chickens are associated with accumulation of large volumes of ascites sometimes as high as 1 L (Tiwari et al., 2013). Leghorn chickens exhibit severe dehydration, arched back, altered gait, and cachexia during stages III and IV ovarian cancer, ultimately leading to death. We isolated chicken ovarian cancer (**COVCAR**) cells from ascites and found that the cancer cells are highly invasive when cultured in an extracellular matrix substance. Furthermore, we found that COVCAR cells expressed greater amounts of genes and proteins typically associated with ovarian adenocarcinoma and in ovarian cancer cell lines derived from human subjects (Tiwari et al., 2013, 2014, 2015). Clusters or spheroids of epithelial ovarian cancer cells are typically found in the ascites collected from human subjects (Allen et al., 1987), and such aggregation of cells is necessary for anchorage-independent growth in three-dimension (Kantak and Kramer, 1998). In addition, ascites-derived spheroids also aid in metastasis of ovarian cancer by implanting on the mesothelium and on the serosal surface of visceral organs (Burleson et al., 2006). Stem cell–like human ovarian cancer cells collected from ascites readily formed aggregates or spheroids in anchorage-independent cultures (Bapat et al., 2005). Based on the foregoing, it is important to understand the biology of ovarian cancer cell spheroids for preventing or limiting the metastasis of ovarian cancer cells.

In the present study, we sought to determine if ovarian cancer stem cells exist in the ascites collected from the chicken model and to determine spheroid formation as well as its invasiveness. We present novel evidence that spheroids formed by the ovarian cancer stem cells isolated from the chicken model possess unique morphological features in forming a network of interconnected structures when cultured over an extended period.

MATERIALS AND METHODS

Animals and Cell Culture

All animal procedures described in this manuscript were approved by the Pennsylvania State University Institutional Animal Care and Use Committee. Female White Leghorn chickens (3–4 yr old; Hyline W36 strain; n = 25) were reared in individual cages at the Poultry Education and Research Center of the Pennsylvania State University and exposed to a photoperiod of 16 h light and 8 h dark. The animals were provided with layer mash diet and water ad libitum. Egg production records were maintained daily to determine ovulatory cycle patterns. Tissue collection and ascites-derived cell culture were done as described previously (Tiwari et al., 2013). Briefly, animals were observed daily for classical signs of ovarian cancer (anovulation, inanition, dehydration, enlarged abdomen, abnormal gait). Animals suspected of having ovarian cancer were euthanized by cervical dislocation. The abdominal cavity was opened aseptically, and the viscera, including ovary, were examined for the presence of tumor mass and metastatic tumor nodules. The entire ovary was then collected and preserved for histopathological analysis and extraction of RNA and protein. Ascites, if present, were collected aseptically and processed immediately. Cells present in ascites were collected by centrifugation at 125 × *g* for 5 min at 25°C (n = 8 animals). Ascites-derived COVCAR cells were resuspended in MCDB105:M199 (1:1) culture medium (Sigma-Aldrich, St. Louis, MO), containing 10% chicken serum, 5% horse serum, 5% fetal bovine serum (**FBS**; Sigma-Aldrich), L-alanine-L-glutamine dipeptide (Corning, Corning, NY), penicillin-streptomycin-fungizone solution (Invitrogen, Carlsbad, CA) and cultured in 75 cm^2 cell culture flasks at 37°C under 5% CO_2 atmosphere. The cancer cells were allowed to attach while any remaining blood cells, as well as non-adherent cells, were washed away by exchanging cell culture medium a few times. When the cells reached 80-90% confluence, 0.5% trypsin (Invitrogen) solution was applied to dissociate cells and to identify and separate ovarian cancer stem cells.

ALDEFLUOR Assay and Fluorescence-Activated Cell Sorting

Aldehyde dehydrogenase 1 is considered as a marker for stem cells and is present in tumors of several organs, including ovary (Deng et al., 2010; Flesken-Nikitin et al., 2013). Primary COVCAR cells (n = 8 animals) obtained and maintained individually as described previously were subjected to ALDEFLUOR assay (STEMCELL Technologies, Vancouver, Canada) following the manufacturer's protocol. ALDH1 enzyme activity was measured in this assay followed by fluorescence-activated cell sorting (**FACS**) to separate $ALDH1^+$ and $ALDH1^-$ cells. Briefly, COVCAR cells (~5 million cells per mL) were added to ALDEFLOUR reagent (1 µl/10^6 cells) without or with diethylamino benzaldehyde (**DEAB**; an ALDH1 inhibitor added as negative control) and incubated at 37°C for 30 min. After removing the ALDEFLOUR reagent, the cells were suspended in ALDEFLUOR assay buffer and subjected to FACS. Cells with high ALDH1 activity (**$ALDH1^+$**) and low ALDH1 activity (**$ALDH1^-$**) were sorted at 4°C in a Cytopeia Influx cell sorter (BD Biosciences, San Jose,

CA) and collected into serum-free stem cell medium [**SCM**; X-VIVO 20 medium (Lonza, Walkersville, MD) supplemented with 5 μg/mL bovine insulin (Sigma-Aldrich), 20 ng/mL recombinant human epidermal growth factor (PeproTech, Rocky Hill, NJ), and penicillin-streptomycin-fungizone solution (Invitrogen)].

Three-Dimensional Anchorage-Independent Culture of ALDH1$^+$ and ALDH1$^-$ Cells

ALDH1$^+$ and ALDH1$^-$ cells were plated (10,000 cells per well; n = 8 animals) immediately after FACS in 24-well ultralow attachment plates (Corning) in serum-free SCM and incubated at 37°C under 5% CO_2 atmosphere for 6 D. Both ALDH1+ and ALDH1− cell wells were visualized using an Axioskop microscope (Zeiss, New York, NY) and photographed using Axiocam digital camera (Zeiss) every day for the determination of spheroid formation. On day 6, the number of spheroids (50 μm or larger in diameter) was counted in non-overlapping fields in all wells using an Axioskop microscope (Zeiss). To determine if spheroids exhibited further growth, incubation was continued for 1–6 mo. Spheroids were transferred individually, aided by stereomicroscope, to fresh culture medium every week using sterile glass capillary tubes used for embryo transfer or 1 mL plastic syringes and photographed periodically.

Matrigel Invasion Assay

The upper chamber of transmembrane cell culture inserts (BD Biosciences) having 8 μm pores was coated with 200 μl Matrigel extracellular matrix (2 mg/mL; BD Biosciences) in serum-free SCM and allowed to solidify at 37°C under 5% CO_2 for 2 h. Approximately 40,000 ALDH1+ and ALDH1$^-$ cells (n = 4 animals) in serum-free SCM were layered on the Matrigel-coated insert, which was suspended into one of a 24-wells plate containing 750 μl of X-VIVO 20 culture medium containing 10% chicken serum. Plates were then incubated at 37°C under 5% CO_2 atmosphere for 24 h. After incubation, cells remaining in the Matrigel layer on the upper surface of the inserts were removed using cotton swabs. Cells that had invaded the Matrigel layer and reached the lower surface of the insert were fixed in methanol and stained with Giemsa stain. The lower surface of the insert was photographed (100x magnification), and the number of invaded cells was counted and averaged from 6 non-overlapping fields per insert (n = 8 animals) by 2 observers.

Di-I Acetylated LDL Assay

Spheroids were transferred to serum-free SCM containing 10 μg/mL DiI conjugated acetylated low-density lipoprotein (**DiI-acLDL**; Invitrogen) and incubated for 4 h at 37°C under 5% CO_2. Spheroids were then washed in phosphate-buffered saline and visualized using an Axioskop fluorescent microscope for determination of cellular uptake of acetylated LDL. To visualize nuclei of the cells in the spheroids, 0.1 μg/mL 4′,6-diamidino-2-phenylindole (**DAPI**; Invitrogen) was added to the culture medium.

Statistical Analysis

Counts of spheroids formed by ALDH1$^+$ and ALDH1$^-$ cells as well as counts of ALDH1$^+$ and ALDH1$^-$ cells invaded through the Matrigel extracellular matrix were analyzed by Student's t-test. A probability value of <0.01 was considered statistically significant.

RESULTS

Gross Morphology and Histology of Ovarian Cancer

We observed that 8 of 25 chickens (32%) developed ovarian cancer. A complete hierarchy of preovulatory and prehierarchical follicles was observed in normal hens (Figure 1A). By contrast, most of the ovarian follicles were atretic in chickens that had ovarian tumor and the ovarian stroma was replaced by a solid tumor mass (Figure 1B). Histological evaluation of the ovarian tissue by hematoxylin and eosin revealed the presence of primary follicles in the ovarian stroma in normal animals (Figure 1C). However, the stroma of ovarian tumor was infiltrated by nests of epithelial cells, forming multiple acini and ductular structures typically found in endometrioid type of ovarian adenocarcinoma (Figure 1D). All 8 animals that developed ovarian cancer had ascites (0.5-1 L) that served as a source for COVCAR cells. In a previous report (Tiwari et al., 2013), we found that ascites-derived COVCAR cells expressed several genes and proteins typically associated with ovarian adenocarcinoma, and therefore, it is assumed that COVCAR cells are likely to originate from ovarian tumor.

Identification and Isolation of ALDH1$^+$ Cells From Ascites-Derived Chicken Ovarian Cancer Cells

Using ALDEFLOUR assay and subsequent fluorescence-activated cell sorting, ALDH1$^+$ and ALDH1$^-$ cell populations were sorted based on the ALDH1 activity. The proportion of ALDH1$^+$ cells in 5–20 million COVCAR cells sorted from each animal ranged between 0.043 and 4.75% with the median proportion of 1.1% (Figure 2B; n = 8 animals). The addition of DEAB to inhibit ALDH1 activity resulted in the separation of fewer cells that were positive for ALDH1 (Figure 2A).

ALDH1$^+$ Cells Are More Invasive Than ALDH1$^-$ Cells

ALDH1$^+$ cells were found to be more invasive than ALDH1$^-$ cells through the Matrigel layer (Figure 2C, E, F). The number of ALDH1$^+$ cells found in the lower

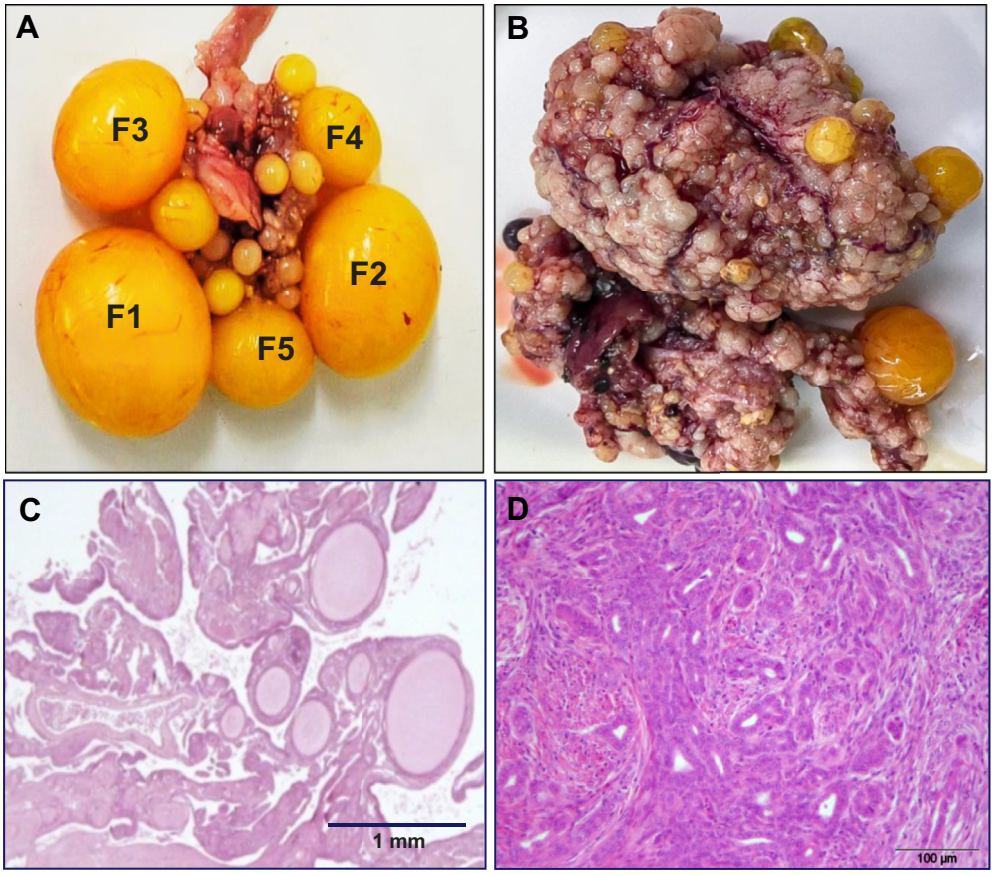

Figure 1. Morphology and histology of normal ovary and ovarian tumor. (A) Normal ovary containing a hierarchy of preovulatory follicles (F1–F5) and prehierarchical follicles. (B) Tumor mass and a few atretic follicles. (C–D) Photomicrograph of hematoxylin- and eosin-stained ovarian tissue sections. (C) Normal ovarian stroma showing homogenous staining pattern and several primary follicles. (D) Cancerous ovarian stroma infiltrated by neoplastic epithelial cells forming multiple acini and ducts.

surface of the membrane was approximately 6-fold greater than that of ALDH1$^-$ cells (Figure 2C; $P = 0.006$).

Anchorage-Independent Culture of ALDH1$^+$ and ALDH1$^-$ Cells

Spheroid Counts We observed that ALDH1$^+$ cells isolated from the ascites of all the chickens (n = 8) that developed ovarian cancer formed spheroids. At the end of 6 D of anchorage-independent culture, the number of spheroids formed by ALDH1$^+$ cells was approximately 5-fold greater than that of ALDH1$^-$ cells (Figure 2D, G, H; $P = 0.005$). ALDH1$^+$ cells readily formed spheroids within 24 h after placing single cells in culture medium, whereas ALDH1$^-$ cells were much slower, requiring at least 48 h after plating to form spheroids. Furthermore, spheroids formed by ALDH1$^+$ cells were larger in size when compared with spheroids formed by ALDH1$^-$ cells (Figure 2G and H). Spheroids formed by ALDH1$^-$ cells were unviable and readily disassociated within 6 D after plating single cells. By contrast, ALDH1$^+$ spheroids remained intact for several months, as evidenced by progressive growth in size, reaching >200 µm and morphological changes that occurred over time. In addition, we observed that only a few ALDH1$^+$ cells remained individually after several days in culture. Enzymatic dissociation of spheroids and subsequent culture of dispersed cells in serum-free SCM lead to reaggregation and formation of spheroids (data not shown).

Interconnected Spheroids

The morphological features of spheroids formed by ALDH1$^+$ cells were found to be unique (Figure 3A–L). Immediately after plating in serum-free culture medium, the single cells (Figure 3A) either started aggregating into smaller clusters or started dividing and organizing cells into a single-file "chain" of cells (Figure 3B). In many of the spheroids formed by ALDH1$^+$ cells, numerous translucent vesicles were observed, as depicted in Figure 3B and C. A long but slender capillary-like tubule was observed extending from the cytoplasm of a single cell (Figure 3C). In addition, spheroids appear to give rise to capillary-like tubules within a few days of culturing single ALDH1$^+$ cells. The tubular formation appeared to follow 3 distinct processes: (1) budding cells from the surface of the spheroid (Figure 3E, K), (2) by sprouting tubules (Figure 3F, G, I), or (3) by both budding and sprouting (Figure 3H). The core of some of the spheroids appears to contain highly coiled, narrow semitranslucent tubule (Figure 3L). Approximately 75% of the spheroids (data not shown) formed out of ALDH1$^+$ cells isolated from

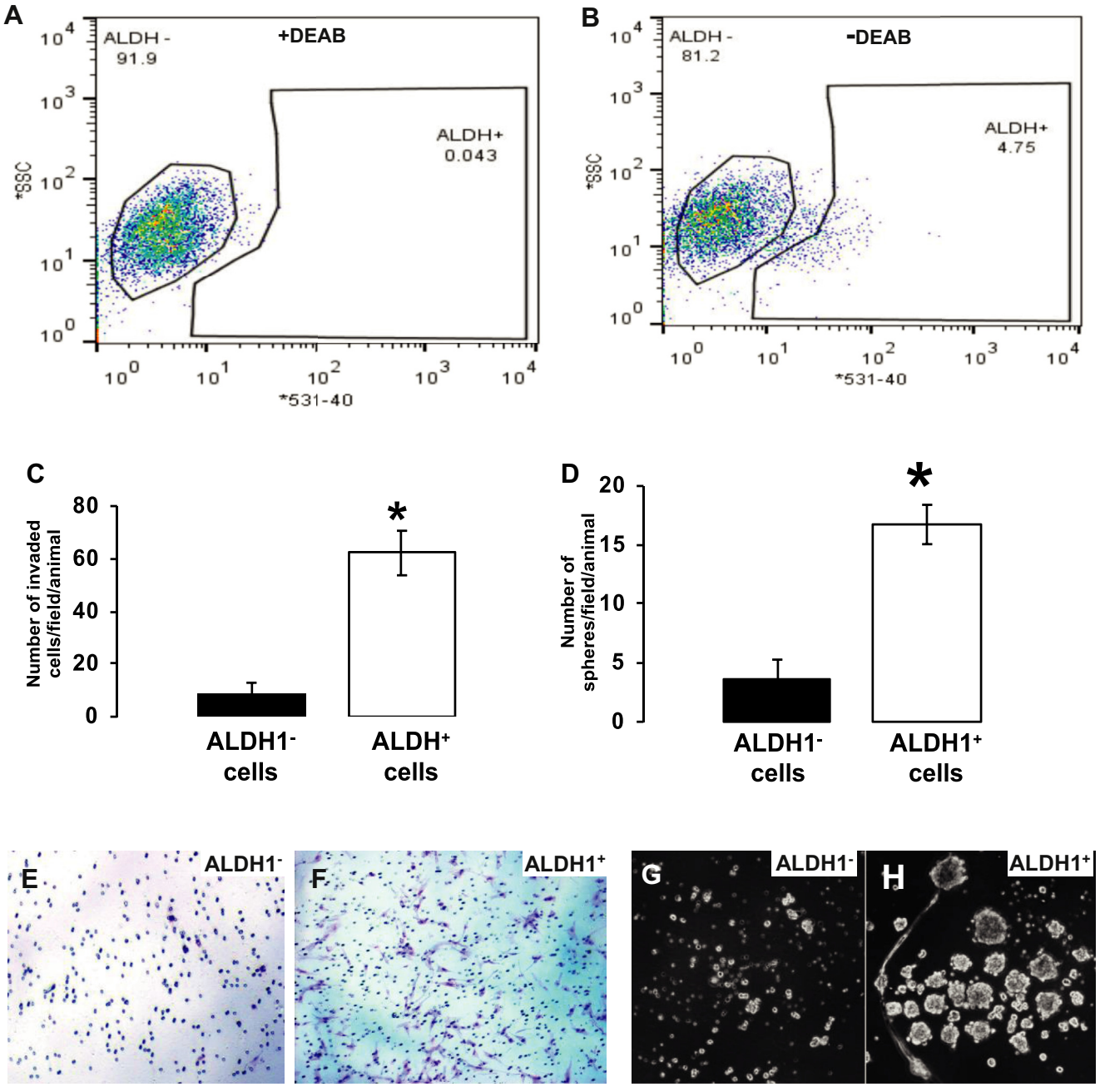

Figure 2. (A–B) Graphical representation of fluorescence-activated sorting of ALDH1$^+$ and ALDH1$^-$ cells. Ascites-derived primary ovarian cancer cells in their first passage were subjected to ALDEFLOUR assay to sort cells based on aldehyde dehydrogenase 1 (ALDH) activity. Assay specificity was determined by the addition or omission of diethylamino benzaldehyde (DEAB), an inhibitor of ALDH (A, B). (C, E, F) Matrigel invasion assay of ALDH1$^+$ and ALDH1$^-$ cells. ALDH1$^+$ and ALDH1$^-$ cells were layered on top of solidified Matrigel in transmembrane insert having 8 μm pores and cultured for 24 h as described in *Materials and Methods* section. The number of ALDH1$^+$ and ALDH1$^-$ cells invaded through the Matrigel and pores were counted in 6 fields after staining the bottom surface of the membrane (C; $*P < 0.001$; n = 4 animals). Representative photomicrographs of the membrane bottom surface, showing many ALDH1$^+$ cells (F) while ALDH1$^-$ cells were a few in number (E). (D, G, H) Spheroid formation property of ALDH1$^+$ and ALDH1$^-$ cells in anchorage-independent culture. ALDH1$^+$ and ALDH1$^-$ cells (10,000 cells per well) were plated in serum-free stem cell culture media in ultra-low attachment plate and incubated at 37°C. On day 6 of culture, the number of spheres (≥50 μm diameter) were counted in non-overlapping fields (D; $*P < 0.01$; n = 8 animals). Representative photomicrographs of spheres formed by ALDH1$^+$ cells (G) and ALDH1$^-$ cells (H).

ascites of all animals (n = 8) developed tubules of varying length and complexity.

We observed that many spheroids, when allowed to grow in 3-D culture, have connected themselves through single or multiple tubules (Figure 4A-G). In some samples, we observed that multiple clusters of cells appeared along the length of the tubules (Figure 4A, F), while the tubules in others remained free of such small-cell clusters (Figure 4B, G). In Figure 4E, the terminal end of the tubule seems to have a "tip-cell" that appears to be guiding the formation of the tubule. Instead of a single cell, a cluster of cells was found at the terminal end of the tubule as seen in Figure 4C and F. We also observed microtentacles-like structure protruding from the surface of some tubules that seemingly attempt to connect to adjacent structures (Figure 4D). Multiple capillary-like tubules, when traversing through a spheroid, were found to be highly coiled, giving a braided-appearance (Figure

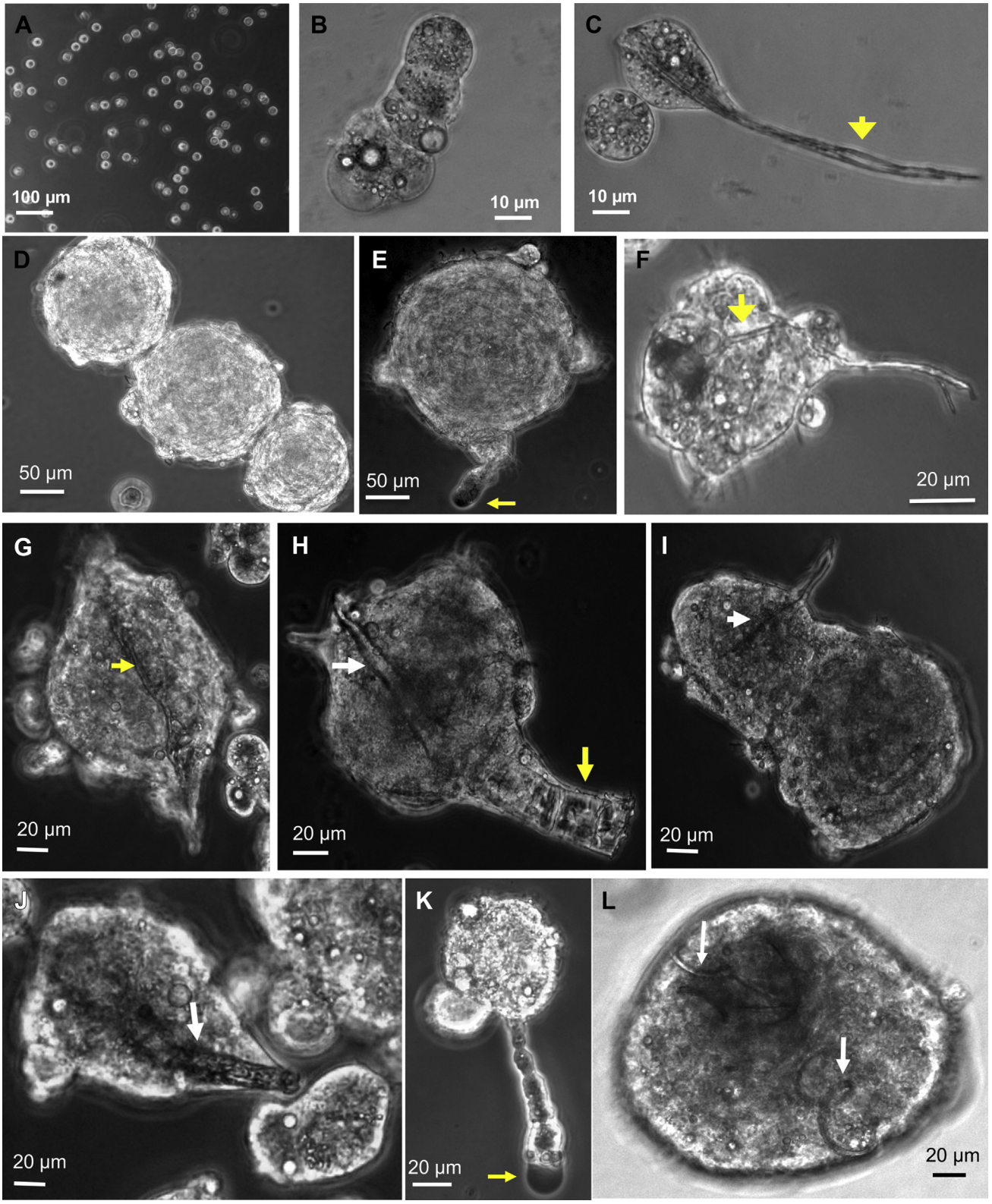

Figure 3. (A–L) Representative phase-contrast photomicrographs of spheroids formed by ALDH1$^+$ cells. ALDH1$^+$ ovarian cancer stem cells were sorted using ALDEFLOUR assay and fluorescence-activated cell sorting from cultures of ascites-derived primary ovarian cancer cells (passage #1). ALDH1$^+$ cells were cultured in ultralow attachment plates in serum-free stem cell media containing epidermal growth factor and insulin. The cells appeared as singlets immediately after plating (A) but assembled into clusters (B) or capillary-like tubes (C; arrow). Within a few days, several spheroids were formed (D–L). Note budding of cells from the surface of the spheroids (yellow arrows in E, H, and K). Capillary-like tubules can be visualized on the surface of the spheroid (arrows in F and G) or in the spheroid core (white arrows in H, I, J, and L). Some of the tubules appear coiled (as in L) and traverse the core of the entire spheroid (n = 8 chickens).

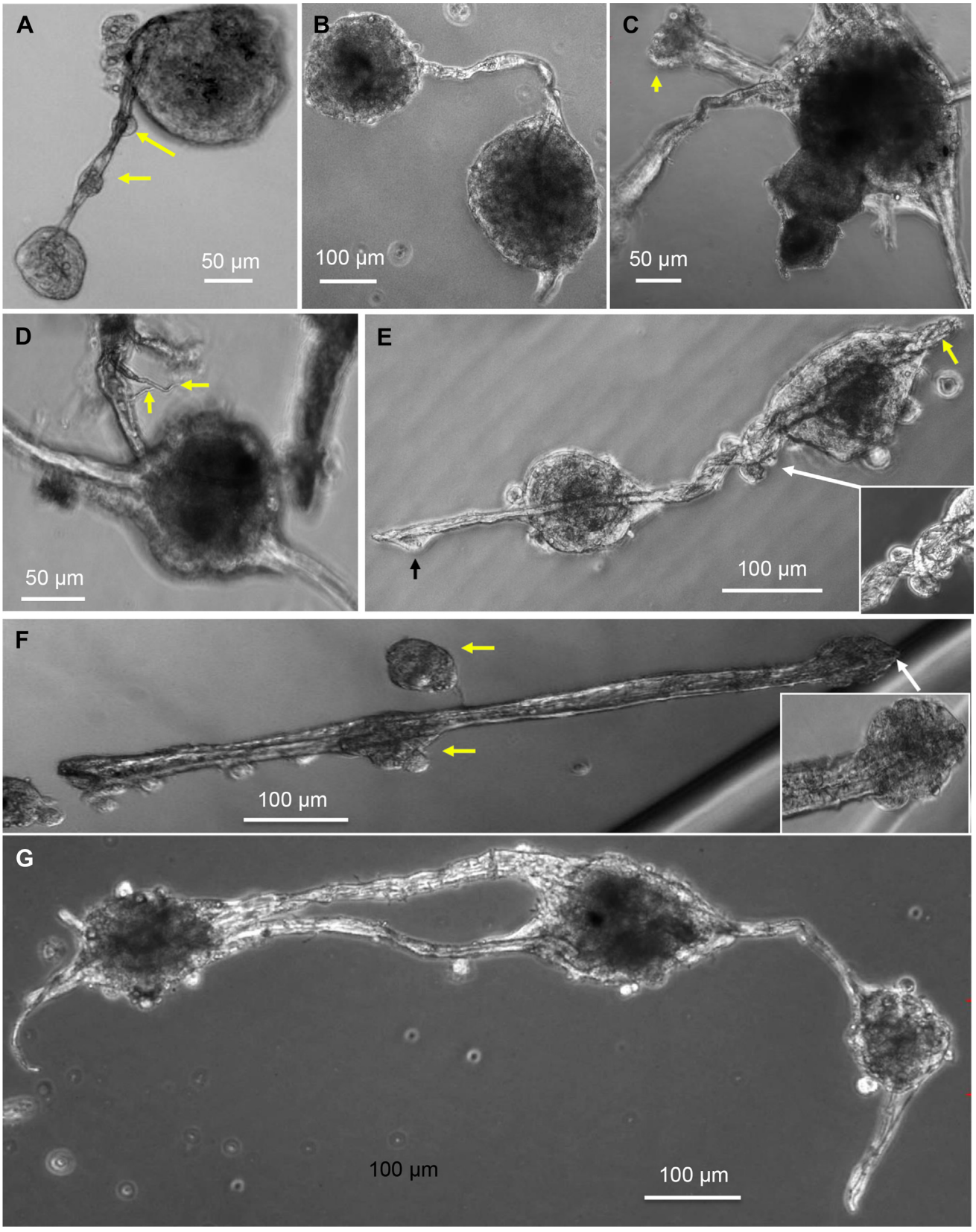

Figure 4. (A–G) Representative phase-contrast photomicrographs of interconnected. spheroids and spheroids. ALDH1^{+} ovarian cancer stem cells were cultured as described in Figure 2 legend. Capillary-like translucent tubules were found to connect spheroids (A, B, E, and G). Arrows in A indicate the presence of cells along the length of the tubule. A spheroid with multiple dense spheroids with associated tubules is shown in C. Arrow in C indicates a cluster of cells at the terminal end of the tubule. Microtentacles-like tiny tubules can be seen sprouting from a larger tubule (arrows in D). A tip cell at the terminal end of the tubule is visualized in E (black arrow). Several tubules found coiled together, forming a braided-bundle of tubule in E (yellow arrow and see *inset* for magnified image). A long (~1 mm) tube (F) with multiple spheroids attached (yellow arrow). One end of the tubule is embedded into a spheroid (white arrow; see *inset* for magnified image). One of the longest and complex structures with 3 spheroids and associated tubules is depicted in G (n = 8 chickens).

4E). As seen in Figure 3, the tubules greatly varied in length. One of the linear capillary-like tubules with multiple clusters of cells along its length was determined to be at least 800 μm in length and was visible to the naked eye (Figure 4F). Upon examining at a higher magnification, this tubule is connected to a spheroid by a slender stalk (Figure 4F). We observed that some of the spheroids are almost opaque, possibly revealing higher cellularity within them (Figure 4B, C, D). Stereomicroscopic images of the spheroids reveal that some parts of the tubules are translucent, while others are covered with rough deposits on the surface (Figure 5A-F). The terminal end of some of the tubules has clusters of cells (Figure 5A). Documented observations of spheroid growth reveal that the spheroids underwent remodeling over a period of time. Time-lapse images of 3 representative spheroids (Figure 6) depict significant structural changes that occurred over 2–17 wk of three-dimensional culture in the absence of extracellular matrix.

Spheroids Incorporate Di-I acLDL

Several constituent cells of the spheroids incorporated DiI-acLDL suggestive of scavenger receptor activity in the cells (Figure 7B). The nuclei of constituent cells in

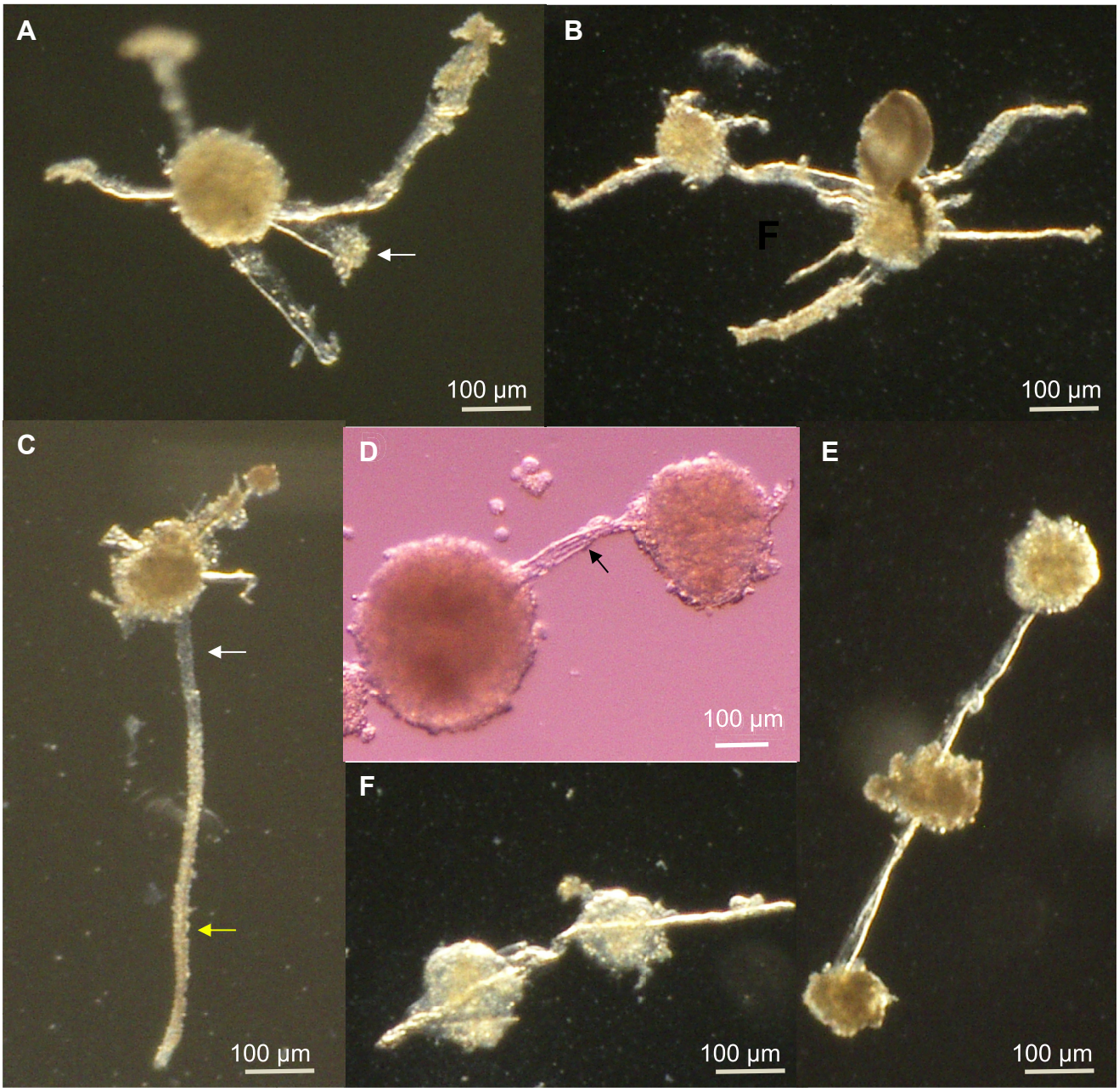

Figure 5. (A–F) Representative stereomicroscopic photomicrographs of spheroids. ALDH1$^+$ ovarian cancer stem cells were cultured as described in Figure 2 legend. Some spheroids (as in A, C) never connected to another spheroid but sprouted multiple tubules that appeared translucent (white arrow in C) in some areas. The surface of the tubule appeared rough in some areas (yellow arrows in C). Two or more spheroids are connected by one or more tubules, as seen in B, D, E, and F. Arrow in D points to the presence of multiple distinct tubules that connect 2 spheroids (n = 8 chickens).

the spheroid can be visualized as blue (DAPI) staining (Figure 7A).

DISCUSSION

This is the first report to document the existence of ovarian cancer stem cells in a naturally occurring ovarian cancer animal model. Our data suggest that ALDH1$^+$ cells constitute a small proportion (0.043–4.75%) of the primary ovarian cancer cell population present in ascites. Consistent with our results, ALDH1$^+$ ovarian cancer stem cells were found in ascites and in ovarian tumor tissue in human subjects, although there were significant variations in their abundance (0.25–7.78% in ovary and 1.5%-39.30% in ascites (Silva et al., 2011)). We also found that ALDH1$^+$ cells were more invasive than ALDH1$^-$ cells when cultured on Matrigel. This is consistent with the invasive properties of ALDH1$^+$ cells isolated from human ovarian cancer cell lines (Kuroda et al., 2013). ALDH1$^+$ cells present in human ovarian cancer cell lines were highly tumorigenic upon xenotransplantation (Kuroda et al., 2013; Yasuda et al., 2013). Knockdown of ALDH1 gene expression resulted in a reduced number of invading renal cell carcinoma cells when subjected to invasion assay (Wang et al., 2013). Our data also suggest that ALDH1$^+$ cells exhibited greater sphere formation than ALDH1$^-$ cells consistent with previous reports on human ovarian cancer cell lines (Wang et al., 2012; Kuroda et al., 2013). ALDH1^{low} cells isolated from high-grade serous ovarian and clear cell carcinoma cell lines Greater sphere formation ability has been observed in ALDH1^{high} cancer stem cells compared to (Kuroda et al., 2013)

We present novel evidence that the ovarian cancer spheroids continued to grow and give rise to a complex network of tubules. A three-dimensional culture system devoid of extracellular matrix or scaffolds allowed us to document morphological changes occurring in aggregates of ovarian cancer stem cells over an extended period. Some of these tubules were as long as 1 mm and 25–30 μm in diameter and were even visible to the naked eye. The formation of capillary-like tubules observed in the present study is reminiscent of a phenomenon termed as vascular mimicry displayed by aggressive cancer cells. Vascular mimicry involves the generation of acellular microvascular channels lined by aggressive tumor cells without the participation of endothelial cells or existing blood vessels (Maniotis et al., 1999). Vascular mimicry

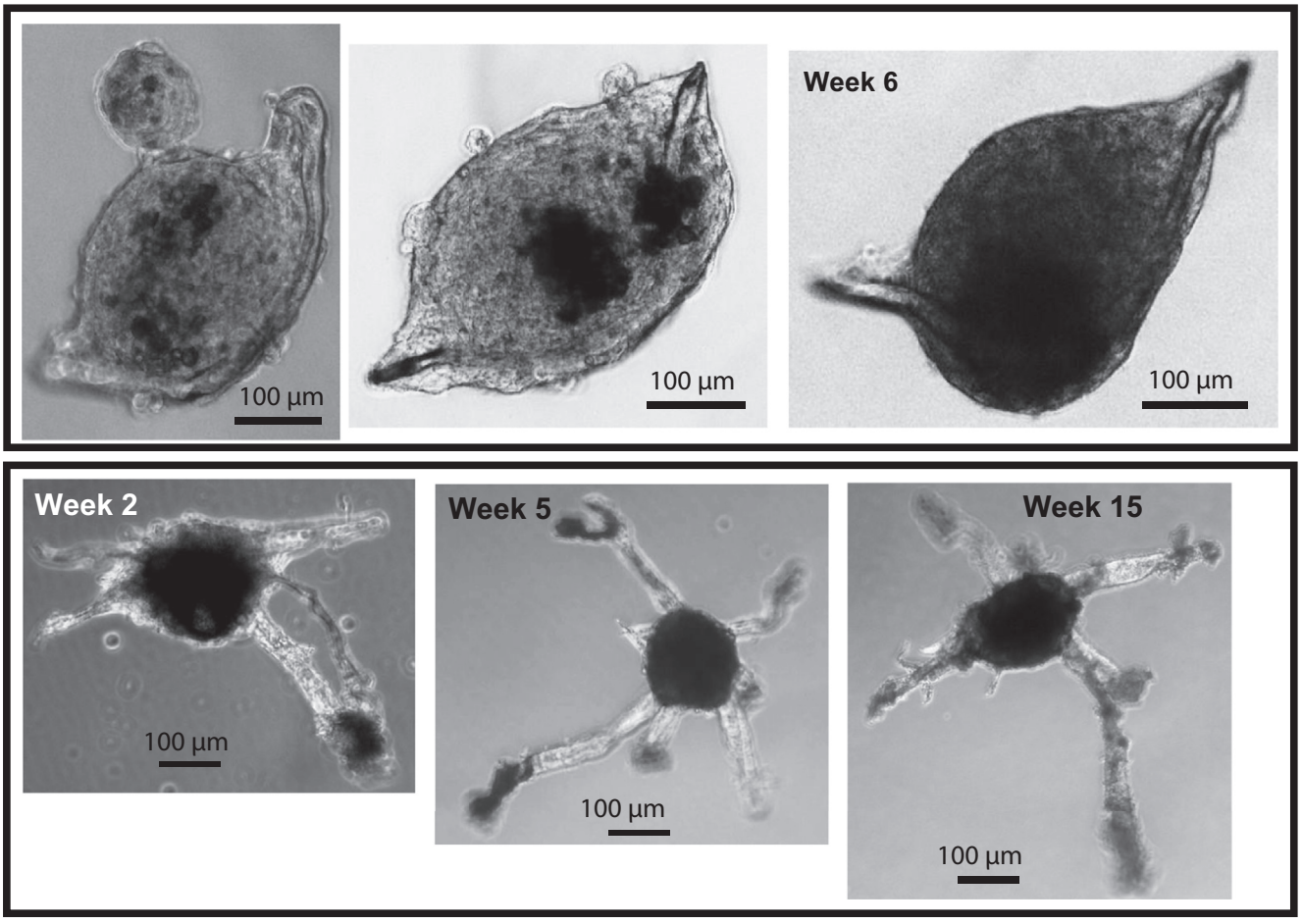

Figure 6. Time-lapse phase-contrast photomicrographs of representative spheroids studied over a 1- to 17-wk period. ALDH1$^+$ ovarian cancer stem cells were cultured as described in Figure 2 legend. Upper and lower panels depict 2 spheroids undergoing morphological changes over time. Notice a gradual increase in cellularity within the spheroid (top panel) at 2, 3, and 6 wk in culture. Tubular remodeling in a spheroid observed on 2, 5, and 15 wk in culture (lower panel).

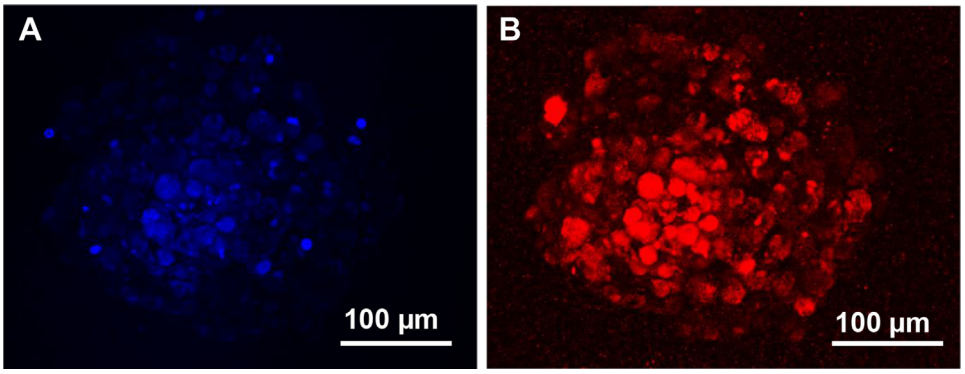

Figure 7. (A–B) Representative photomicrographs of ALDH1$^+$ spheroids showing incorporation of DiI-acLDL. ALDH1$^+$ ovarian cancer stem cells were cultured as described in Figure 2 legend. Spheroid was incubated with DiI-acLDL and DAPI for 4 h and washed. Cells that have incorporated DiI-acLDL appear red (B) while the cell nuclei, stained by DAPI, appear blue (A) (n = 8 chickens).

channels consisting of solid but hollow tubes were found to be developed by culturing highly invasive melanoma cells in Matrigel or collagen (Maniotis et al., 1999). In addition to aggressive melanoma cells, several cell lines derived from breast cancer (Liu et al., 2013), hepatocellular carcinoma (Sun et al., 2013), and ovarian cancer (Alvero et al., 2009; Su et al., 2011; Du et al., 2014) were found to exhibit vascular mimicry channels when cultured in collagen or basement matrix. Aggressive ovarian cancer cell lines such as OVCAR3 and SKOV3, when grown in 3-dimensional culture in the presence of Matrigel, developed hollow vascular mimicry channels composed of extracellular matrix and lined by tumor cells (Sood et al., 2001). In addition to aggressive cancer cells, endothelial cells derived from umbilical veins form spheroids and angiogenic sprouts when cultured in collagen (Heiss et al., 2015). Based on our data, ovarian cancer stem cells isolated from the chicken model appear to be unique among other cancer cells in that they form complex networks of capillary-like tubules in the absence of extracellular matrix and that these tubules connect multiple spheroids.

Based on the foregoing, we hypothesize that the tubules connecting multiple spheroids are potentially transporting molecules from one spheroid to the other and thus serve as an intraspheroidal channel. In support of this theory, the existence of nanoscale conduits or nanoscale membrane bridges that transfer miRNA and exosomes from metastatic breast cancer cells to endothelial cells have been reported (Connor et al., 2015). Similar intercellular communication channels were found to transfer exosomes from melanoma cells to bone marrow progenitor cells (Peinado et al., 2012). Both the chemical and structural composition of the tubules and their function remain to be elucidated.

We observed that some of the tubules appear to sprout from the core of the spheroid. Considering the size of the spheroid (>100 μm), the core is likely to be hypoxic, which may contribute to the formation and sprouting of tubules. In support of this theory, hypoxic microenvironment has been found to promote vascular mimicry by activating transcription factors favoring cell survival, migration, and angiogenesis. Chemically induced hypoxia by treatment with cobalt chloride and subsequent activation of hypoxia-inducible factor-1-alpha promotes vascular mimicry in matrix-supported three-dimensional culture of ovarian cancer cells by inducing epithelial-mesenchymal transition (Du et al., 2014). OVCAR3 cells are also reported to form vessel-like networks that also expressed CD31 and vascular endothelial–cadherin (Su et al., 2011). In addition to hypoxia, several growth factors have been found to promote vascular mimicry in cancer cells. Overexpression of human epidermal growth receptor-2 in MCF7 breast cancer cells was found to create vascular mimicry channels in three-dimensional culture (Liu et al., 2013). Similarly, overexpression of snail family transcriptional repressor-2 induces vascular mimicry in HepG2 and Huh-7 hepatocellular carcinoma cell lines (Sun et al., 2013). When cultured in extracellular matrix, ovarian cancer cells acquire vascular endothelial–cadherin, and this process may require inhibitor of kappa β but not vascular endothelial growth factor to induce formation of vascular mimicry channels (Alvero et al., 2009). In summary, most aggressive cancer cells appear to have angiogenic properties.

Our data suggest that many of the cells in the spheroids have incorporated DiI-acLDL, indicating the existence of scavenger receptor activity, typically observed in endothelial cells and microglial cells (Voyta et al., 1984). This suggests that ovarian cancer stem cells may have differentiated into endothelial cells. Patient-derived organoids that contain cancer stem cells and differentiated cells have been developed recently from hepatocellular carcinoma (Broutier et al., 2017), breast cancer (Sachs et al., 2018), glioblastoma (Hubert et al., 2016), and pancreatic cancer (Seino et al., 2018). Such organoids are promising tools for understanding cancer genetics and for determining drug sensitivity *in vitro* as they represent the native tumor environment. Further studies are required to determine if the spheroids of ovarian cancer stem cells observed in the present study recapitulate the histological and molecular signature of ovarian tumor, the hallmarks of cancer organoids.

In summary, our study suggests that highly invasive cancer stem cells exist in the ascites collected from the

chicken model of spontaneous ovarian adenocarcinoma. The ovarian cancer stem cells organize into spheroids and develop complicated networks of capillary-like tubules reminiscent of vascular mimicry. Our data further prove that the chicken model of ovarian cancer can be very useful in improving our understanding of the biology of cancer stem cells. In addition, isolation and characterization of chicken stem cells would also help to advance our knowledge on ovarian function and egg production. Furthermore, a clear understanding of the ovarian cancer cells would help to prevent ovarian cancer incidence and improve the welfare of Leghorn chickens.

ACKNOWLEDGMENTS

This project was supported in part by grant number 1R03 CA208573 from the National Cancer Institute at the National Institutes of Health. The authors thank Ruth Nissly and Ningchun Xu of the Microscopy and Cytometry Facility in the Huck Institute of the Life Sciences for their assistance in fluorescence-activated cell sorting.

REFERENCES

Allen, H. J., C. Porter, M. Gamarra, M. S. Piver, and E. A. Johnson. 1987. Isolation and morphologic characterization of human ovarian carcinoma cell clusters present in effusions. Exp. Cell Biol. 55:194–208.

Alvero, A. B., H. H. Fu, J. Holmberg, I. Visintin, L. Mor, C. C. Marquina, J. Oidtman, D. A. Silasi, and G. Mor. 2009. Stem-like ovarian cancer cells can serve as tumor vascular progenitors. Stem Cells. 27:2405–2413.

Bapat, S. A., A. M. Mali, C. B. Koppikar, and N. K. Kurrey. 2005. Stem and progenitor-like cells contribute to the aggressive behavior of human epithelial ovarian cancer. Cancer Res. 65:3025–3029.

Barnes, M. N., W. D. Berry, J. M. Straughn, T. O. Kirby, C. A. Leath, W. K. Huh, W. E. Grizzle, and E. E. Partridge. 2002. A pilot study of ovarian cancer chemoprevention using medroxyprogesterone acetate in an avian model of spontaneous ovarian carcinogenesis. Gynecol. Oncol. 87:57–63.

Barua, A., P. Bitterman, J. S. Abramowicz, A. L. Dirks, J. M. Bahr, D. B. Hales, M. J. Bradaric, S. L. Edassery, J. Rotmensch, and J. L. Luborsky. 2009. Histopathology of ovarian tumors in laying hens: a preclinical model of human ovarian cancer. Int. J. Gynecol. Cancer. 19:531–539.

Broutier, L., G. Mastrogiovanni, M. M. Verstegen, H. E. Francies, L. M. Gavarro, C. R. Bradshaw, G. E. Allen, R. Arnes-Benito, O. Sidorova, M. P. Gaspersz, N. Georgakopoulos, B. K. Koo, S. Dietmann, S. E. Davies, R. K. Praseedom, R. Lieshout, I. J. JNM, S. J. Wigmore, K. Saeb-Parsy, M. J. Garnett, L. J. van der Laan, and M. Huch. 2017. Human primary liver cancer-derived organoid cultures for disease modeling and drug screening. Nat. Med. 23:1424–1435.

Burleson, K. M., M. P. Boente, S. E. Pambuccian, and A. P. Skubitz. 2006. Disaggregation and invasion of ovarian carcinoma ascites spheroids. J. Transl. Med. 4:6.

Campbell, J. G. 1951. Some unusual gonadal tumours of the fowl. Br. J. Cancer. 5:69–82.

Connor, Y., S. Tekleab, S. Nandakumar, C. Walls, Y. Tekleab, A. Husain, O. Gadish, V. Sabbisetti, S. Kaushik, S. Sehrawat, A. Kulkarni, H. Dvorak, B. Zetter, R. E. Edelman, and S. Sengupta. 2015. Physical nanoscale conduit-mediated communication between tumour cells and the endothelium modulates endothelial phenotype. Nat. Commun. 6:8671.

Deng, S., X. Yang, H. Lassus, S. Liang, S. Kaur, Q. Ye, C. Li, L. P. Wang, K. F. Roby, S. Orsulic, D. C. Connolly, Y. Zhang, K. Montone, R. Butzow, G. Coukos, and L. Zhang. 2010. Distinct expression levels and patterns of stem cell marker, aldehyde dehydrogenase isoform 1 (ALDH1), in human epithelial cancers. PloS One. 5:e10277.

Du, J., B. Sun, X. Zhao, Q. Gu, X. Dong, J. Mo, T. Sun, J. Wang, R. Sun, and Y. Liu. 2014. Hypoxia promotes vasculogenic mimicry formation by inducing epithelial-mesenchymal transition in ovarian carcinoma. Gynecol. Oncol. 133:575–583.

Fathalla, M. F. 1971. Incessant ovulation a factor in ovarian neoplasia? Lancet. 2:163.

Flesken-Nikitin, A., C. I. Hwang, C. Y. Cheng, T. V. Michurina, G. Enikolopov, and A. Y. Nikitin. 2013. Ovarian surface epithelium at the junction area contains a cancer-prone stem cell niche. Nature. 495:241–245.

Fredrickson, T. N. 1987. Ovarian tumors of the hen. Environ. Health Perspect. 73:35–51.

Heiss, M., M. Hellstrom, M. Kalen, T. May, H. Weber, M. Hecker, H. G. Augustin, and T. Korff. 2015. Endothelial cell spheroids as a versatile tool to study angiogenesis in vitro. FASEB J. 29:3076–3084.

Hubert, C. G., M. Rivera, L. C. Spangler, Q. Wu, S. C. Mack, B. C. Prager, M. Couce, R. E. McLendon, A. E. Sloan, and J. N. Rich. 2016. A three-dimensional organoid culture system derived from human glioblastomas recapitulates the hypoxic Gradients and cancer stem cell Heterogeneity of tumors found in vivo. Cancer Res. 76:2465–2477.

Johnson, P. A., and J. R. Giles. 2013. The hen as a model of ovarian cancer. Nat. Reviews. Cancer. 13:432–436.

Jordan, C. T., M. L. Guzman, and M. Noble. 2006. Cancer stem cells. N. Engl. J. Med. 355:1253–1261.

Kantak, S. S., and R. H. Kramer. 1998. E-cadherin regulates anchorage-independent growth and survival in oral squamous cell carcinoma cells. J. Biol. Chem. 273:16953–16961.

Kuroda, T., Y. Hirohashi, T. Torigoe, K. Yasuda, A. Takahashi, H. Asanuma, R. Morita, T. Mariya, T. Asano, M. Mizuuchi, T. Saito, and N. Sato. 2013. ALDH1-high ovarian cancer stem-like cells can be isolated from serous and clear cell adenocarcinoma cells, and ALDH1 high expression is associated with poor prognosis. PloS One. 8:e65158.

Lengyel, E., J. E. Burdette, H. A. Kenny, D. Matei, J. Pilrose, P. Haluska, K. P. Nephew, D. B. Hales, and M. S. Stack. 2014. Epithelial ovarian cancer experimental models. Oncogene. 33:3619–3633.

Lingeman, C. H. 1974. Etiology of cancer of the human ovary: a review. J. Natl. Cancer Inst. 53:1603–1618.

Liu, T., B. Sun, X. Zhao, Q. Gu, X. Dong, Z. Yao, N. Zhao, J. Chi, N. Liu, R. Sun, and Y. Ma. 2013. HER2/neu expression correlates with vasculogenic mimicry in invasive breast carcinoma. J. Cell. Mol. Med. 17:116–122.

Maniotis, A. J., R. Folberg, A. Hess, E. A. Seftor, L. M. Gardner, J. Pe'er, J. M. Trent, P. S. Meltzer, and M. J. Hendrix. 1999. Vascular channel formation by human melanoma cells in vivo and in vitro: vasculogenic mimicry. Am. J. Pathol. 155:739–752.

Peinado, H., M. Aleckovic, S. Lavotshkin, I. Matei, B. Costa-Silva, G. Moreno-Bueno, M. Hergueta-Redondo, C. Williams, G. Garcia-Santos, C. Ghajar, A. Nitadori-Hoshino, C. Hoffman, K. Badal, B. A. Garcia, M. K. Callahan, J. Yuan, V. R. Martins, J. Skog, R. N. Kaplan, M. S. Brady, J. D. Wolchok, P. B. Chapman, Y. Kang, J. Bromberg, and D. Lyden. 2012. Melanoma exosomes educate bone marrow progenitor cells toward a pro-metastatic phenotype through MET. Nat. Med. 18:883–891.

Sachs, N., J. de Ligt, O. Kopper, E. Gogola, G. Bounova, F. Weeber, A. V. Balgobind, K. Wind, A. Gracanin, H. Begthel, J. Korving, R. van Boxtel, A. A. Duarte, D. Lelieveld, A. van Hoeck, R. F. Ernst, F. Blokzijl, I. J. Nijman, M. Hoogstraat, M. van de Ven, D. A. Egan, V. Zinzalla, J. Moll, S. F. Boj, E. E. Voest, L. Wessels, P. J. van Diest, S. Rottenberg, R. G. J. Vries, E. Cuppen, and H. Clevers. 2018. A Living Biobank of breast cancer organoids Captures disease Heterogeneity. Cell. 172:373–386.e310.

Seino, T., S. Kawasaki, M. Shimokawa, H. Tamagawa, K. Toshimitsu, M. Fujii, Y. Ohta, M. Matano, K. Nanki, K. Kawasaki, S. Takahashi, S. Sugimoto, E. Iwasaki, J. Takagi, T. Itoi,

M. Kitago, Y. Kitagawa, T. Kanai, and T. Sato. 2018. Human pancreatic tumor organoids reveal Loss of stem cell niche factor Dependence during disease progression. Cell Stem Cell. 22:454–467 e456.

Silva, I. A., S. Bai, K. McLean, K. Yang, K. Griffith, D. Thomas, C. Ginestier, C. Johnston, A. Kueck, R. K. Reynolds, M. S. Wicha, and R. J. Buckanovich. 2011. Aldehyde dehydrogenase in combination with CD133 defines angiogenic ovarian cancer stem cells that portend poor patient survival. Cancer Res. 71:3991–4001.

Sood, A. K., E. A. Seftor, M. S. Fletcher, L. M. Gardner, P. M. Heidger, R. E. Buller, R. E. Seftor, and M. J. Hendrix. 2001. Molecular determinants of ovarian cancer plasticity. Am. J. Pathol. 158:1279–1288.

Steg, A. D., K. S. Bevis, A. A. Katre, A. Ziebarth, Z. C. Dobbin, R. D. Alvarez, K. Zhang, M. Conner, and C. N. Landen. 2012. Stem cell pathways contribute to clinical chemoresistance in ovarian cancer. Clin. Cancer Res. 18:869–881.

Su, M., W. Wei, X. Xu, X. Wang, C. Chen, L. Su, and Y. Zhang. 2011. Role of hCG in vasculogenic mimicry in OVCAR-3 ovarian cancer cell line. Int. J. Gynecol. Cancer. 21:1366–1374.

Sun, D., B. Sun, T. Liu, X. Zhao, N. Che, Q. Gu, X. Dong, Z. Yao, R. Li, J. Li, J. Chi, and R. Sun. 2013. Slug promoted vasculogenic mimicry in hepatocellular carcinoma. J. Cell Mol. Med. 17:1038–1047.

Tiwari, A., J. A. Hadley, G.L. Hendricks, 3rd, R. G. Elkin, T. Cooper, and R. Ramachandran. 2013. Characterization of ascites-derived ovarian tumor cells from spontaneously occurring ovarian tumors of the chicken: evidence for E-cadherin upregulation. PloS One. 8:e57582.

Tiwari, A., J. A. Hadley, and R. Ramachandran. 2014. Aquaporin 5 expression is altered in ovarian tumors and ascites-derived ovarian tumor cells in the chicken model of ovarian tumor. J. Ovarian Res. 7:99.

Tiwari, A., O. M. Ocon-Grove, J. A. Hadley, J. R. Giles, P. A. Johnson, and R. Ramachandran. 2015. Expression of adiponectin and its receptors is altered in epithelial ovarian tumors and ascites-derived ovarian cancer cell lines. Int. J. Gynecol. Cancer. 25:399–406.

Voyta, J. C., D. P. Via, C. E. Butterfield, and B. R. Zetter. 1984. Identification and isolation of endothelial cells based on their increased uptake of acetylated-low density lipoprotein. J. Cell Biol. 99:2034–2040.

Wang, K., X. Chen, Y. Zhan, W. Jiang, X. Liu, X. Wang, and B. Wu. 2013. Increased expression of ALDH1A1 protein is associated with poor prognosis in clear cell renal cell carcinoma. Med. Oncol. 30:574.

Wang, Y. C., Y. T. Yo, H. Y. Lee, Y. P. Liao, T. K. Chao, P. H. Su, and H. C. Lai. 2012. ALDH1-bright epithelial ovarian cancer cells are associated with CD44 expression, drug resistance, and poor clinical outcome. Am. J. Pathol. 180:1159–1169.

Yasuda, K., T. Torigoe, R. Morita, T. Kuroda, A. Takahashi, J. Matsuzaki, V. Kochin, H. Asanuma, T. Hasegawa, T. Saito, Y. Hirohashi, and N. Sato. 2013. Ovarian cancer stem cells are enriched in side population and aldehyde dehydrogenase bright overlapping population. PloS One. 8:e68187.